Experimental Investigation of Enhanced Shroud Flange Designs for Improved Urban Wind Turbine Performance in Low-Wind Conditions

Ali Niknahad[1], Abdolamir Bak-Khoshnevis[1*], Morteza Abdolzadeh[2]

[1] Department of Mechanical Engineering, Hakim Sabzevari University, Sabzevar, Iran
[2] Department of Mechanical Engineering, Kerman Graduate University of Technology, Kerman, Iran

Abstract:

The growing demand for sustainable energy highlights the need for efficient small-scale wind turbines, especially in urban areas with low wind speeds and limited space. This study experimentally examines aerodynamic augmentation effects on turbine performance using shrouds and tailored flanges. Four turbine configurations—a bare turbine, a turbine with a simple shroud, a shroud with a vertical flange, and a shroud with an improved curved flange—were three-dimensional printed and tested in a controlled wind tunnel under realistic low- to moderate-speed urban wind conditions. Airflow velocity at the shroud throat and corresponding power output were measured across various wind speeds. Results show that both flange curvature and height significantly affect aerodynamic performance. The curved-flange design consistently increased throat velocity and turbine output, achieving up to a 32.3-fold power gain over the bare turbine at 5 m/s. At higher wind speeds, differences among augmented configurations decreased, yet the improved curved flange still delivered approximately 4.3 times the output of the bare turbine at 16.35 m/s. These findings emphasize the importance of outlet geometry in lowering startup thresholds, sustaining airflow acceleration, and maximizing energy capture. Overall, this study provides robust experimental evidence that shrouds with improved curved flanges significantly enhance small-scale urban wind turbine efficiency, offering a practical solution for low-wind energy harvesting and guiding future designs for improved performance across diverse wind regimes.

Keywords: Shroud; flange; wind turbine; computational fluid dynamics; wind tunnel; experimental approach

Email: khoshnevis@hsu.ac.ir

1. Introduction

The transition to sustainable energy is not merely an ecological obligation but a strategic imperative to ensure the long-term prosperity of future generations. By reducing greenhouse gas emissions and decreasing dependence on nonrenewable energy sources, alternative energy systems play a crucial role in preserving finite resources. Among these, wind energy has emerged as a leading solution, with wind turbines and related technological advancements gaining widespread adoption. However, to maximize energy capture and improve system efficiency, turbine designs must be carefully improved. In particular, the integration of aerodynamically refined components has consistently demonstrated the potential to reduce operational costs while enhancing power output. Consequently, aerodynamic optimization and the incorporation of advanced structural configurations are essential in the development of turbine shrouds, key elements in wind energy systems, especially within urban settings.

This study builds on recent advancements in turbine shroud research, both air-driven and water-driven, offering foundational context for the present investigation. Modifying the geometry of turbine enclosures and introducing innovative structural features are central strategies for improving wind energy harvesting. As global energy demands continue to grow, expanding the use of wind power becomes increasingly vital.

Aranake et al. [1] conducted experimental and computational analyses of turbine enclosures, emphasizing their role in enhancing energy generation. In a subsequent study, Aranake and Duraisamy [2] investigated how different shroud geometries affect airflow over turbines, employing rotationally symmetric simulations of annular structures modeled with high-lift airfoil profiles. Dilimulati et al. [3] demonstrated

that diffuser-equipped shrouds can effectively guide and accelerate wind flow over buildings, significantly improving the power coefficient of conventional turbines.

In the context of water-based turbines, Shahsavarifard and Bibeau [4] observed that off-axis wind conditions under yaw angles reduce energy conversion efficiency, highlighting the importance of precise turbine alignment. Siavash et al. [5] introduced a partially open conduit design that outperformed conventional shrouds in terms of energy extraction and rotor speed, particularly under high wind conditions. This design also reduced structural resistance, thereby improving overall turbine efficiency.

Other enhancements include the use of guide vanes, lobed ejectors, and diffusers integrated into the turbine– shrouds system. Karmakar and Chattopadhyay [6] noted that vertical-axis wind turbines are particularly well-suited for urban areas due to their adaptability and performance in turbulent airflow conditions. Ilhan et al. [7] described diffuser-augmented wind turbines as advanced systems capable of improving wind speed and energy extraction efficiency by factors of 1.5 and 3.38, respectively.

Bontempo and Manna [8] critically evaluated diffuser-augmented wind turbines (DAWTs), focusing on the design of enclosures for existing open-blade rotors. Through numerical simulations, they examined the aerodynamic performance of an NREL Phase VI rotor enclosed in a ring-shaped shroud based on the Selig S1223 airfoil. Their analysis covered key aerodynamic parameters, including blade surface pressure, velocity profiles, aerodynamic forces, tip vortex behavior, and wake dynamics.

Additional design elements, such as pre-swirl vanes, have been shown to modify inflow characteristics by increasing tangential force on turbine blades, thereby boosting energy output. Han et al. [9] demonstrated that combining a turbine enclosure with a lobed ejector reduced rear exit pressure, leading to increased power generation. Similarly, Kosasih and Tondelli [10] showed that a simple conical diffuser could significantly enhance the performance of small-scale wind turbines by increasing optimal blade rotational speed.

In moderate wind environments, incorporating a diffuser into the turbine structure can significantly enhance energy capture. Pambudi et al. [11] found that a diffuser without an entry enclosure could accelerate wind flow by approximately 10%, while combining a diffuser with an inlet enclosure increased flow velocity by up to 13.3%. Al-Quraishi et al. [12] demonstrated that Diffuser Augmented Wind Turbines (DAWTs) can notably boost power generation, particularly in small-scale urban turbines, when the diffuser is properly designed. Beyond performance benefits, diffuser-based shrouds also contribute to noise reduction and provide protective shielding for turbine blades.

Akour and Abo Mhaisen [13] further emphasized that increasing the average inlet velocity to the turbine could amplify power generation by a factor of 4.3 compared to an unshielded turbine. These findings underline the critical role of aerodynamic enhancement in optimizing turbine efficiency.

Efforts to refine turbine enclosure and flange structures have shown promising results in boosting energy output. Leloudas et al. [14] proposed a modular design framework using a synchronized Differential Evolution algorithm to optimize the aerodynamic shape of diffuser-supported turbine enclosures. This approach led to the development of an improved enclosure profile (SD2), which, although thicker than its predecessor (SD1), maintained comparable aerodynamic performance. Both designs achieved significant volume reductions and corresponding increases in wind velocity.

Ohya et al. [15] showed that a diffuser-equipped turbine featuring a flanged enclosure could outperform an uncovered turbine. In this configuration, the flange also functioned as a rudder, helping the turbine align with incoming wind. Building on this concept, Niknahad and Khoshnevis [16] investigated the aerodynamic optimization of shroud flanges by transforming a straight vertical flange into various curved profiles. Their study demonstrated that optimizing flange curvature could enhance mean airflow velocity through the shroud by up to 20%. Additionally, the optimized flange intensified vortex formation behind the shroud, reducing downstream pressure and increasing turbulent kinetic energy levels. These results

established a foundational basis for future refinements in flange design aimed at improving turbine performance in low-wind urban environments.

Further performance improvements can be achieved by adjusting turbine positioning and incorporating multiple rotor systems. While enclosure structures enhance efficiency, they also introduce higher rotor loads. To address this, Lipian et al. [17] proposed the use of an additional rotor to distribute aerodynamic forces more evenly across the system, thus improving overall performance. Subsequent simulations by Lipian et al. [18] validated this concept, showing that twin-rotor configurations reduce the airflow burden on the primary turbine, leading to more balanced and efficient operation.

Research in wind turbine advancement continues to evolve, with numerous studies focused on performance-enhancing strategies. Amin et al. [19], in their study "Evaluation of Variables Affecting Savonius Wind Turbine Efficiency," examined the operational principles and design optimizations of vertical-axis Savonius turbines. Their work highlighted key performance metrics such as torque and power coefficients, which are essential for evaluating turbine efficiency.

A multidisciplinary approach has also been applied to the development of enclosed turbines. Notably, Hosseini and Saboohi [20], in their comprehensive review "Enclosed Wind Turbines: A Review of Design Variations," investigated the transformative potential of ducted wind turbines (DWTs) as an advancement over traditional horizontal-axis wind turbines (HAWTs). Their study analyzed four distinct DWT configurations, offering valuable insights into performance efficiency, economic viability, operational lifespan, and environmental impact.

In another study, Maftouni and Taghaddosi [21] presented "A CFD Study of a Flanged Shrouded Wind Turbine: Effects of Different Flange Surface Types on Output Power." Using computational fluid dynamics (CFD), they investigated the influence of flange surface types, simple versus furrowed, on turbine performance. All models maintained identical inlet and outlet diameters, diffuser lengths, and flange heights, differing only in surface geometry. The results, validated against experimental data,

indicated that furrowed flange surfaces improved airflow velocity near the blades, leading to a 5–7% increase in power output. Moreover, the study found that peak wind velocity occurs approximately 5 cm downstream from the shroud entrance, suggesting an optimal turbine placement for maximum energy capture.

Hu and Wang [22], in their work "Upgrading a Shrouded Wind Turbine with a Self-Adaptive Flanged Diffuser," proposed an innovative self-adaptive flange for wind turbines equipped with flanged diffusers. This adaptive design aims to reduce wind loads at high wind velocities while preserving aerodynamic benefits under rated conditions. Through fluid-structure interaction simulations, the study evaluated how the flange dynamically adjusts its structure in response to wind speed. The results showed that the adaptive flange design could reduce the total wind load on the diffuser by approximately 35% at wind speeds of 60 m/s, significantly improving structural resilience without compromising performance at lower wind speeds.

Significant advancements have been made in the field of wind turbine noise reduction and performance optimization. With rising household energy demands, it is increasingly important to develop strategies that enhance wind turbine efficiency, particularly in urban environments. This study addresses that challenge by introducing streamlined, high-efficiency geometries designed to optimize the performance of small-scale urban wind turbines. All components were fabricated via 3D printing and evaluated in a controlled wind tunnel environment, where their aerodynamic and energy performance were rigorously tested under realistic low-wind conditions. While previous studies have primarily explored the use of diffusers, guide vanes, and simple flange structures to enhance airflow and power generation, the novelty of the current research lies in the design and experimental evaluation of curved flange geometry specifically developed for turbine enclosures. The aerodynamic performance of this enhanced geometry was verified through wind tunnel experiments, ensuring reliable data under real-world low-wind urban conditions. Although various studies have investigated the enhancement of wind turbine performance using diffusers, lobed ejectors, and conventional flanges, most have been limited to simple structural

modifications or computational modeling without comprehensive experimental validation. This study addresses that gap by introducing a curved-flange design aimed at improving airflow at the turbine throat and by evaluating its aerodynamic and energy performance exclusively through experimental testing. By focusing on low-speed urban wind conditions, employing a refined aerodynamic shroud, and providing thorough experimental verification, this work significantly contributes to improving the efficiency and practical viability of small-scale wind turbines in urban environments, advancing beyond the capabilities demonstrated in previous studies.

2. Methodology and Geometry

This study investigates the effect of enhanced curvature in wind turbine shroud flanges to improve wind acceleration within the enclosure. The results presented in this study are based on the numerical data obtained by Niknahad and Khoshnevis [16]. The research focuses on experimentally evaluating the airflow behavior influenced by the shroud geometry and systematically modifying the flange structure, including adjustments to the curvature angle and height. The objective is to identify the configuration that provides the greatest increase in air velocity at the throat of the shroud under controlled laboratory conditions. Fig. 1(a) presents a three-dimensional model of the shroud with a vertical flange attached to its end. In this design, the inlet diameter is 5.20 cm, the total length of the shroud is 22.71 cm, the height of the baseline flange is 1.90 cm, and the outlet diameter is 6.41 cm. Following the design recommendations of Gish et al. [23], the NACA 0006 airfoil profile was used to form the cross-section of the shroud. This aerodynamic configuration is expected to enhance flow guidance and ultimately improve the turbine's power output based on the experimental observations. The improved curved-flange configuration was developed to further intensify the flow acceleration through the shroud. As illustrated in Fig. 1 (b), the enhanced flange replaces the straight wall with a smoothly bent arc defined by a curvature length of 6.9 cm. The curved profile redirects the flow outward and forms an inclination of approximately 37° relative to the axial centerline. This geometry establishes a more pressure difference between inlet and outlet of the shroud, and guides the accelerated jet more effectively toward the turbine

rotor plane. The arc was constructed using two boundary points—the shroud exit and the terminal point of the curve—connected through a continuously varying curvature. The curved flange enables the core stream to contract more sharply toward the throat region, thereby enhancing velocity amplification compared with the baseline design.

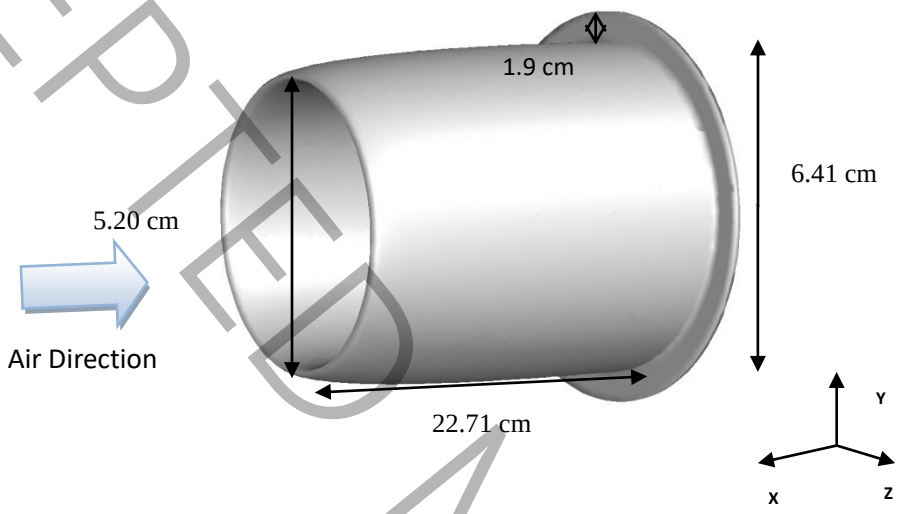

(a)

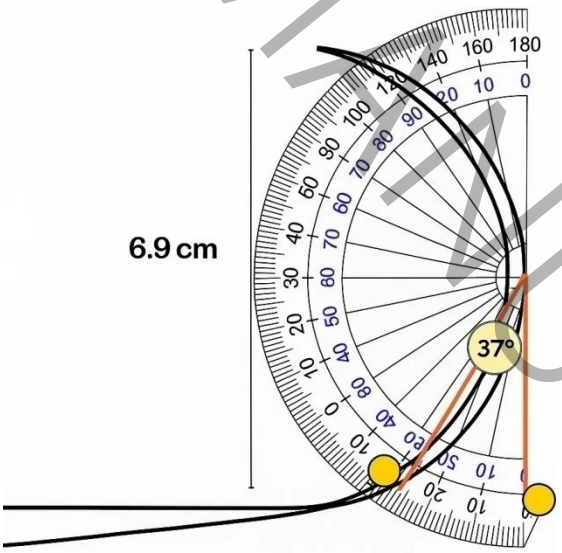

(b)

Fig.1 (a) Angled visualization of the shroud with the flange connected at its terminal, (b) Improved Curved-Flange Configuration.

The experimental procedure is summarized below:

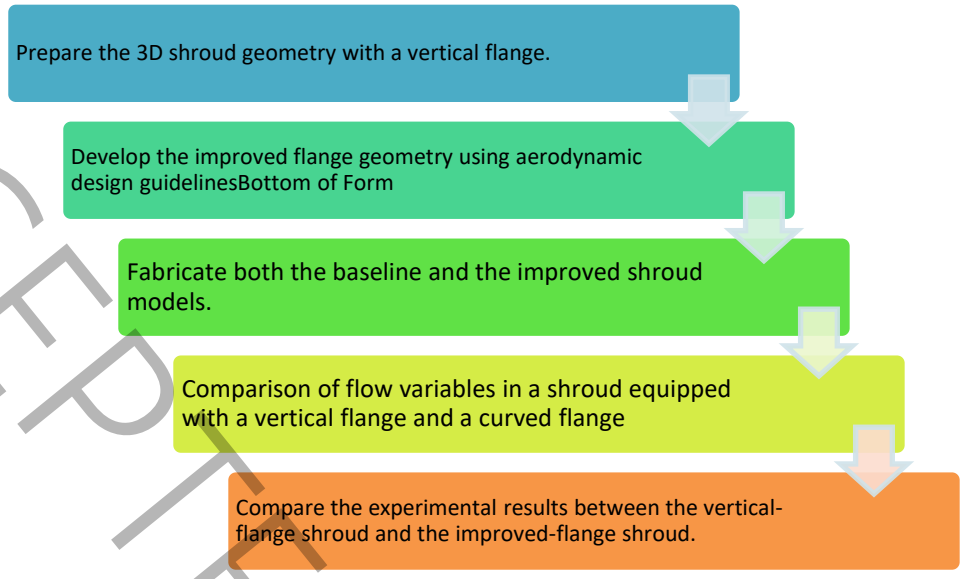

3. Experimental Arrangement

A series of experiments were conducted in the Aerodynamics Laboratory at Hakim Sabzevari University to evaluate the aerodynamic performance of different shroud configurations. The wind tunnel, powered by a 110 kW three-phase electric motor, can generate airflow velocities up to 50 m/s. To ensure uniform and laminar flow at the entrance of the test section, the tunnel is equipped with a honeycomb nylon flow straightener followed by three additional layers of nylon screens, as shown in Fig. 3. The experimental setup included a three-phase generator, rheostat, pitot tube, manometer, voltmeter, and ammeter. Figs. 2(a) and (b) show the wind tunnel, which provides a maximum airflow speed of 50 m/s and features a test chamber with dimensions of 2 m × 1 m × 1 m. The blockage ratio in the test section was kept at approximately 7%. Initially, the shroud without any flange or turbine was placed in the wind tunnel, and the airflow velocity at the throat was measured at various incoming wind speeds. The vertical and curved flanges were then installed on the shroud, and the same measurements were repeated. No turbine was present during these flow-field measurements. Subsequently, turbine-performance experiments were performed. First, the turbine alone (without any shroud or augmentation device) was mounted in the wind tunnel, and its power output was measured under different loads and wind speeds using a rheostat to apply controlled electrical loading. The turbine was then placed inside a plain shroud (without flanges) and tested again. Afterwards, the turbine was sequentially installed inside the shroud with a vertical flange

and then the curved flange, and the same measurement protocol was followed for each configuration. To minimize the influence of structural supports on the results, only a single belt was used to hold the shroud, and the supports were positioned so that they did not significantly disturb the boundary layer. Due to the short length of the shroud, no noticeable vibration occurred during testing. Additionally, dampers were installed between the plexiglass test section and the wind tunnel structure to prevent transmission of environmental vibrations and ensure measurement accuracy. Wind speed measurements were obtained using a pitot tube connected to a digital manometer, ensuring accurate airflow velocity readings. The SG6040 airfoil was used for the blade root and the SG6043 airfoil for the blade tip. Each blade was 150 mm long, with a 50 mm hub diameter and a hub length of 60 mm, as shown in Fig. 2(d). A three-blade turbine with a constant 5° pitch angle from root to tip was used. Fig. 2(e) shows the Fara Sanjesh Saba Digital Manometer (Model 2243), which features an accuracy of ±0.1% full scale, a response time of 200 ms, and a measurement capability up to 1250 Pa or 50 m/s (with a Pitot tube). The device supports PRESSURE WARE software for recording pressure and velocity distributions, with data transmitted to a computer via an A/D card. Fig. 2(f) illustrates the Pitot tube used for velocity measurements. Fig. 2(g) presents the three-phase micro generator, operating within a voltage range of 3–24 V and currents of 0.1–1 A. It produces three-phase AC output and uses brushless technology for silent and durable performance. Fig. 2(h) shows the PeakMeter PM8233D+ True RMS Digital Multimeter used for electrical measurements, with voltage and current measurement accuracies of ±0.5% and ±1.0%, respectively. Fig. 3 illustrates the wind tunnel layout, the internal components, and the positioning of the turbine model within the test section.

(a)

(b)

(c)

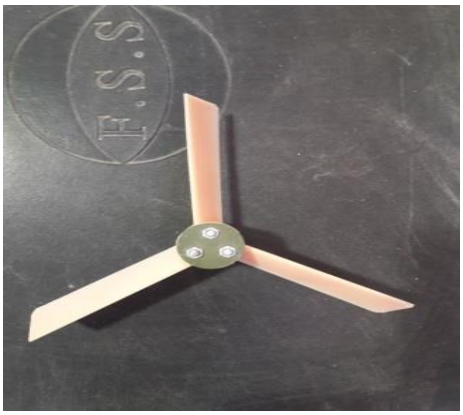

(d)

(e)

(f)

(g)

(h)

Fig. 2 (a) wind tunnel of Hakim Sabzevari University, (b) wind tunnel test section, (c) rheostat, (d) turbine, (e) digital manometer, (f) pitot tube, (g) mini generator, digital multimeter.

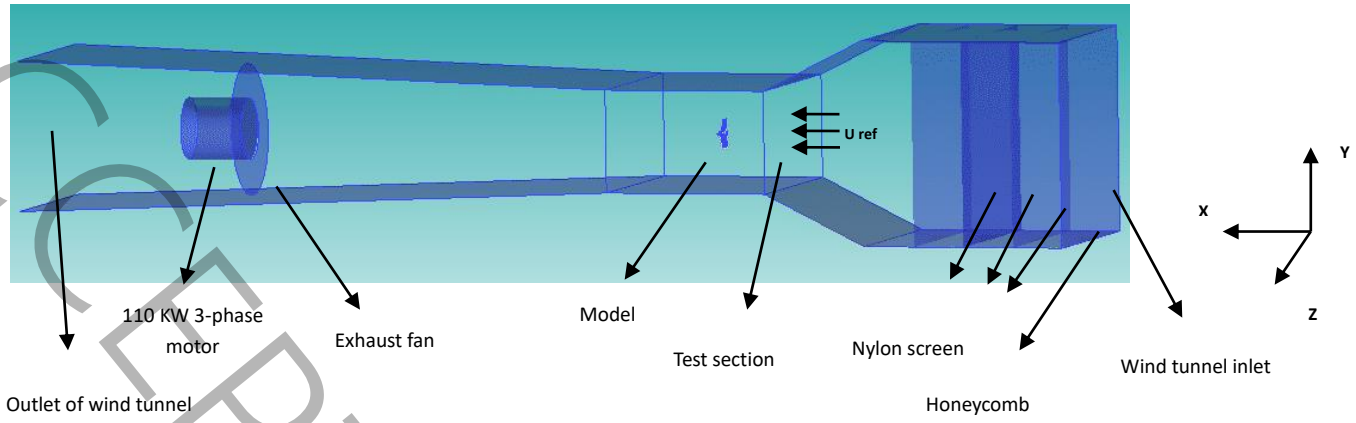

Fig. 3 Schematic of the wind tunnel and its components and the location of the model in the test chamber.

4. Results and Discussion

4-1- Effect of Flange Geometry on Throat Airflow

The effect of flange geometry on airflow through the shroud throat was investigated experimentally. Two shroud configurations were tested: the baseline shroud with a vertical flange, and the improved shroud with the enhanced flange geometry. The improved flange design was developed based on aerodynamic design guidelines and numerical insights from Niknahad and Khoshnevis [16]. Air velocity at the throat will be measured using a pitot tube and a digital manometer, as explained in Section 3. The baseline vertical flange will serve as the reference configuration for comparison. The improved curved flange is expected to produce a higher throat velocity than the baseline, indicating the aerodynamic advantages of the improved flange curvature. The observed trend can be explained by the pressure differences generated by flange curvature. The curved curvature of the improved flange creates a higher pressure gradient between upstream and downstream regions, accelerating airflow through the throat, while the baseline vertical flange produces a lower pressure gradient, resulting in slower airflow. These results confirm that flange curvature is a key factor in determining airflow characteristics and improving turbine performance. The variations in airflow velocity observed between the baseline vertical flange and the improved curved flange translate into meaningful gains in the kinetic energy available to the turbine, given the cubic dependence of power output on wind speed. These findings highlight the importance of carefully

balancing both flange curvature and height to achieve optimal aerodynamic performance and maximize energy yield.

4-2- Analysis of Experimental Measurement Uncertainties

An uncertainty assessment to gauge the reliability of essential experimental readings, specifically wind speed (*U*) and turbine power output (*P*) was performed. Both systematic and random errors were factored into the evaluation, with the overall uncertainty determined using the root-sum-square (RSS) method. The airflow velocity was measured using a Pitot tube connected to a digital manometer manufactured by Farasanjesh Saba Co. According to the manufacturer's specifications, the measurement system has a systematic uncertainty of ±0.1 m/s. This level of accuracy ensures reliable wind speed measurements within the experimental setup. All measurements were conducted after instrument calibration, based on the standard procedures provided by the laboratory. To capture random variations, multiple readings were taken, yielding a standard deviation (σU) of 0.03 m/s. Combining these contributions, the total wind speed uncertainty was computed as $U_{total} = \sqrt{(0.1)^2 + (0.03)^2} = 0.104$ m/s, which corresponds to a relative uncertainty of 1.49%. For turbine power output, measurements relied on voltage (*V*) and current (*I*) via the formula $P = I \times V$. The systematic uncertainties were ±0.02 V for voltage and ±0.005 A for current, while the repeated power readings produced a standard deviation (σP) of 0.03 W. The uncertainty propagation was conducted using the partial derivatives of the power equation with respect to both voltage and current. Under typical operating conditions ($V = 12V$ and $I = 0.5A$), the overall uncertainty was calculated as $U_P = \sqrt{(0.5 \times 0.02)^2 + (12 \times 0.005)^2 + 0.03^2}$, resulting in a relative uncertainty of 1.08%. These findings show that the uncertainties in both wind speed and power output are below 2%, thereby confirming the robustness of the experimental setup. Such minimal uncertainty reinforces the credibility of the turbine performance improvements reported, particularly those attained through the improved shroud and flange design.

4-3- Throat Velocity Measurements and Experimental Repeatability

The performance of three different geometrical configurations—Shroud, Shroud with Vertical Flange, and Shroud with Curved Flange—was investigated under controlled wind tunnel conditions. The experiments were conducted at free stream velocities of 5, 10, and 15 m/s. For each configuration and velocity, five repeated trials were performed to assess the repeatability and consistency of the measurements. From the extracted data (from velocity profiles at the nozzle throat), it is evident that the addition of flanges, particularly the curved flange, significantly enhances the throat velocity compared with the baseline shroud. The measured throat velocities for each trial are presented in Table 1. The results demonstrate a high degree of repeatability, with minimal variation between trials. This indicates that the experimental setup is stable and capable of producing reliable and consistent data across multiple repetitions. Moreover, the incremental increase in throat velocity from the Shroud to the Shroud with Vertical Flange, and finally to the Shroud with Curved Flange, confirms the effectiveness of geometric modifications in enhancing flow acceleration.

Table 1. Throat velocities for five repeated trials under three different geometrical configurations at various free stream velocities.

Free Stream Velocity (m/s)	Geometry	Trial 1	Trial 2	Trial 3	Trial 4	Trial 5
5	Shroud	6.02	5.98	6.05	6.01	6.00
5	Shroud + Vertical Flange	7.01	6.99	7.03	7.02	7.00
5	Shroud + Curve Flange	8.03	7.98	8.01	8.00	8.02
10	Shroud	12.01	12.05	12.00	11.98	12.03
10	Shroud + Vertical Flange	13.02	13.00	13.03	13.01	13.05
10	Shroud + Curve Flange	15.00	15.03	14.98	15.02	15.01
15	Shroud	18.02	18.00	17.98	18.05	18.01
15	Shroud + Vertical Flange	19.50	19.52	19.48	19.51	19.49
15	Shroud + Curve Flange	22.01	22.03	21.98	22.00	22.02

4-4- Tests of Power and Velocity

Fig. 4 displays a schematic of the electrical circuit utilized during the experiments, offering a concise overview of the configuration. Fig. 5 illustrates the connection between the turbine's power output and the free stream velocity (*Uref*) within the wind tunnel test section. Here, power output is determined by the equation $P = I \times V$, where I is the current measured by an ammeter and V is the voltage recorded by a voltmeter. Notably, the turbine remains inactive until the free stream velocity reaches roughly 5 m/s, marking the cut-in speed. At this juncture, wind energy is insufficient to overcome system inertia and associated losses, thus hindering power generation. Once the threshold is exceeded, the power output increases in a non-linear manner with wind speed. This trend aligns with theoretical expectations, as wind turbine power is proportional to the cube of wind speed—a relationship reflected by the steep curve observed in the graph. When the wind speed surpasses 10 m/s, the graph reveals a rapid rise in power output, indicating significantly enhanced performance at higher speeds. This exponential trend further emphasizes the cubic dependency of power on wind speed, demonstrating the turbine's efficiency in converting wind energy into electrical power under optimal conditions. Understanding the interplay between power and velocity is vital for optimizing turbine design and placement. The sharp rise in power output at elevated speeds underscores the importance of situating turbines in areas with consistently strong winds to maximize energy production. Additionally, the marked variations in power and voltage at higher Reynolds numbers hint at the potential need for advanced control strategies to manage power output, thereby protecting electrical components from overload in high-wind conditions.

In this study, all power values have been normalized relative to the maximum power of the standalone turbine at the highest Reynolds number.)

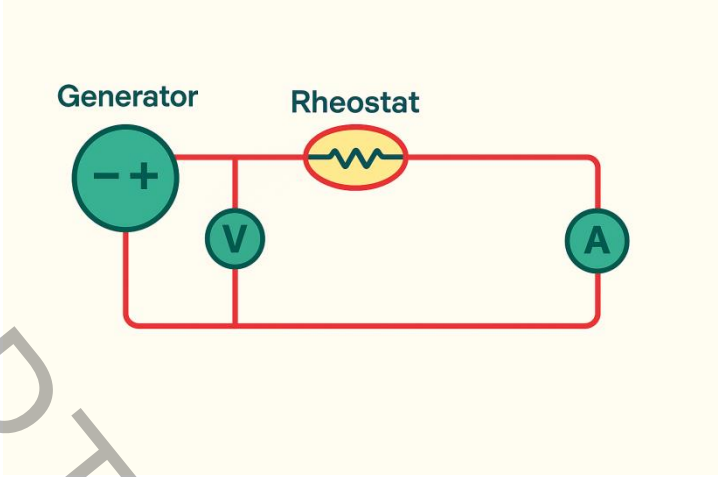

Fig. 4 Schematic of the tested electrical circuit for electrical loading.

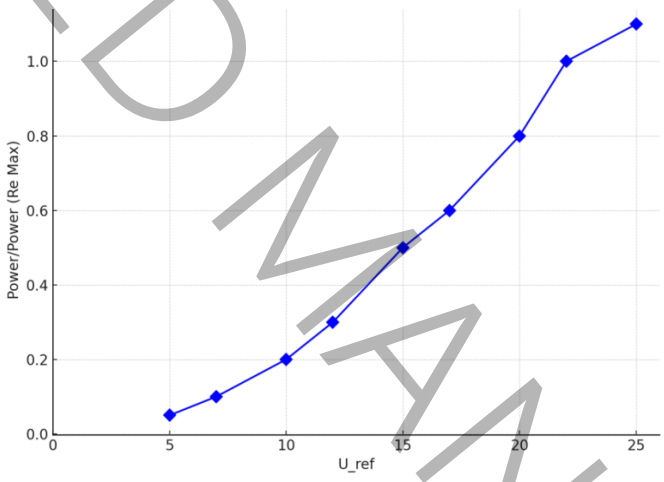

Fig. 5 Turbine power changes with free stream velocity.

4-5- Quantitative Examination of the Power-Voltage Relationship in Context of wind speeds

This investigation provides a numerical evaluation of the relationship between the turbine's energy output and the generator's voltage, highlighting the significant role of wind speed variations. As shown in Fig. 6, the data illustrate how power output evolves with changes in voltage across a range of wind speeds. This study offers valuable insights into the turbine's operational performance under different conditions.

4-6- Peak Power Levels across Varying Wind Speeds

In the presented power-voltage graphs, each curve represents a unique peak power (*Pmax*) occurring at specific voltage points that correspond to different wind speeds. The peak power values observed for these wind speed conditions are detailed in Table 2.

Table 2. Maximum power and voltage at different air speeds

Wind velocity (m/s)	$Pmax/\overline{P\ (Re\ Max)}$	Voltage (V)
6.2	0.004	2.66
10.5	0.122	5.67
13.12	0.261	7.33
16.88	0.526	9.15
20.76	0.859	10.3

The findings establish a clear link between wind speed, Reynolds number, and turbine performance. As wind velocity increases, both the peak power output and the corresponding voltage rise, although this relationship is not linear. In fact, power output accelerates more rapidly at higher wind speeds, suggesting that the turbine operates more efficiently as the Reynolds number increases. An analysis of the power–voltage graphs (Fig. 6) shows that the turbine's response to voltage changes varies with wind speed. For example, at 6.5 m/s, power increases at a relatively gentle rate of about 0.014 (1/V). In contrast, at 20.76 m/s, the power raises much faster—approximately 0.088 (1/V)—indicating that the turbine becomes significantly more sensitive to voltage fluctuations at higher wind speeds, thereby boosting power output per voltage unit. While this increased sensitivity suggests improved efficiency, it also raises the risk of instability if the system is not carefully controlled.

Once the turbine reaches its maximum power at a given wind speed, further increases in voltage lead to a drop in power output. This decline occurs at varying rates depending on the wind speed. For instance, at 13.12 m/s, power decreases from approximately 0.132 to 0.106 as voltage increases from 4.5 V to 6.0 V. Similarly, at 20.76 m/s, power falls more sharply from about 0.256 to 0.230 as voltage rises from 6.8 V to 7.5 V. This more pronounced drop at higher wind speeds highlights the importance of operating near the peak power point to avoid significant performance losses. At very high wind speeds, such as 19.45 m/s and 20.76 m/s, the power curves converge, both reaching a peak power output of approximately 0.256 at similar voltage levels. This convergence suggests that the turbine may be operating at or near its optimal design limits, with diminishing power returns as wind speed increases. This plateau could indicate that the turbine has reached its maximum efficiency or is constrained by mechanical factors.

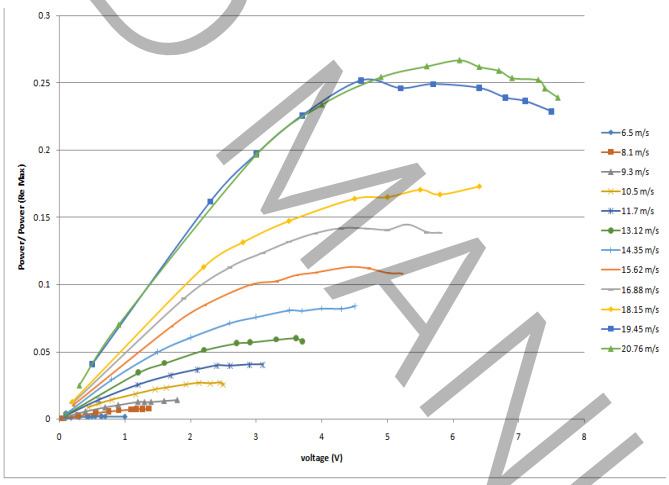

Fig. 6 Variation of turbine power with generator voltage at different wind velocities.

4-7- Shroud Experiments

Fig. 7 shows various augmenter devices and their configurations designed to boost airflow speed within the shroud. The configurations tested include:

- Shroud with turbine only
- Shroud with a vertical flange and turbine

- Shroud with a curved flange and turbine

(a)

(b)

(c)

Fig. 7 a) Shroud + turbine, b) Shroud + vertical flange + turbine, c) Shroud + curved flange + turbine.

Fig. 8 shows that adding a curved flange to the shroud consistently increases throat velocity across all tested free stream wind speeds, outperforming both the shroud-only and vertical flange configurations. While the vertical flange becomes less effective as wind speed increases, the curved flange maintains its performance advantage, making it the most reliable option for enhancing airflow through the shroud.

4-8- Trend Analysis

An analysis of throat velocity trends for different flange configurations reveals several important insights (Fig. 8). In the shroud-only configuration, throat velocity scales linearly with free stream velocity, closely following a 1:1 ratio. This linearity indicates that the shroud alone effectively channels airflow without additional augmentation. However, when a vertical flange is added, the airflow behavior changes. At lower free stream speeds (around 10–12 m/s), the vertical flange enhances throat velocity by approximately 20% and 16.67%, respectively. As wind speed increases to the 14–16 m/s range, this improvement diminishes to about 7.14% and 6.25%, suggesting that the effectiveness of the vertical flange decreases at higher velocities. In contrast, the shroud equipped with a curved flange exhibits consistently superior performance. This configuration maintains a high level of augmentation, with average throat velocity improvements around 50%, and peaking at approximately 56.25% at 16 m/s. These results highlight the curved flange's ability to sustain effective airflow enhancement even as free stream velocity increases. The differences in performance between the three configurations can be explained by their influence on the pressure field and flow structure at the shroud entrance. The vertical flange improves airflow capture at low wind speeds by generating a localized pressure difference that draws more air into the throat. Conversely, the curved flange facilitates a smoother and more gradual flow transition into the shroud. This minimizes separation even at higher wind speeds, which explains its consistent and superior performance across the entire velocity range. The sustained increase in throat velocity with the curved flange confirms that its aerodynamic profile effectively promotes air entrainment and acceleration, making it a robust and reliable design for varying wind conditions.

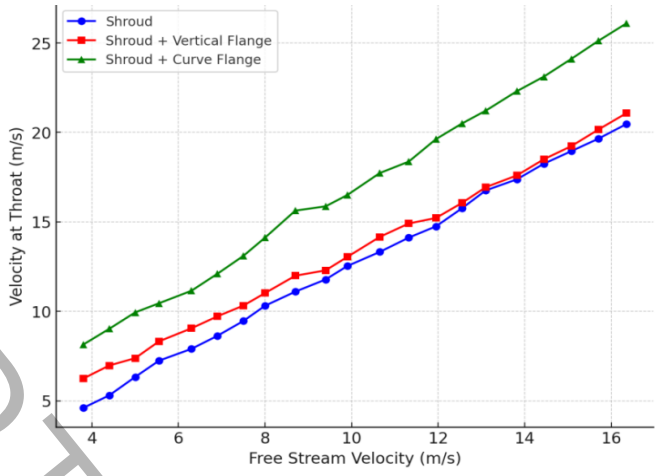

Fig. 8 Velocity variation in shroud throat with air free stream velocity.

4-9- Comparative Performance Insights

A comparison between the two flange types and the baseline shroud-only configuration reveals additional insights. At lower wind speeds, the vertical flange provides moderate to significant improvements in throat velocity, effectively enhancing performance when airflow is relatively weak. However, its effectiveness declines as wind speed increases. In contrast, the curved flange consistently delivers substantial gains across the entire range of tested wind speeds. For instance, at approximately 10 m/s, the vertical flange boosts throat velocity by about 20%, while the curved flange achieves nearly a 50% improvement. At 16 m/s, the vertical flange's enhancement drops to around 6.25%, whereas the curved flange maintains a robust 56.25% increase.

These comparisons clearly highlight the superior aerodynamic performance of the curved flange, particularly at higher wind speeds, reinforcing its value as a more effective and reliable design for enhancing airflow in varying conditions.

4-10- Practical Implications and Recommendations

Based on free stream velocity, the study reveals clear configuration preferences. At low to moderate wind speeds (10–14 m/s), both the vertical and curved flanges enhance throat velocity; however, the curved flange provides a significantly greater increase. When free stream velocities exceed 16 m/s, the performance of the vertical flange declines noticeably, reducing its effectiveness. In contrast, the curved

flange continues to deliver strong performance, indicating that it is the optimal configuration for high-velocity conditions.

4-11- Reliability and Consistency

From a reliability perspective, the curved flange configuration clearly stands out. Its performance remains consistent across varying free stream velocities, ensuring stable turbine operation under a wide range of conditions. This consistency makes the curved flange a more dependable choice when uniform performance is essential. While the vertical flange may perform adequately at lower wind speeds, its diminished effectiveness at higher velocities can result in suboptimal performance, further reinforcing the curved flange's advantage in more demanding scenarios.

4-12- Analysis of Turbine Power with Augmenters

Fig. 9 illustrates the variations in power and current output at free stream velocities of 3.8 m/s, 6.3 m/s, 8.7 m/s, 11.32 m/s, 13.82 m/s, and 16.35 m/s. This analysis provides key insights into how different augmenter configurations affect turbine performance across a realistic range of urban wind speeds. Four configurations were evaluated: a bare turbine, a turbine with a shroud, a turbine with a shroud plus a vertical flange, and a turbine with a shroud plus a curved flange. At wind speeds below 3.8 m/s, the bare turbine produces no power. Even with a shroud, power generation remains minimal. Adding a vertical flange offers a moderate performance improvement, but it is the combination of the shroud and the curved flange that yields a significant power boost—reaching 36.080 units—which represents a dramatic enhancement over all other configurations. This result highlights the critical role of the curved flange in maximizing power generation in low-wind urban environments. As wind speed increases to 6.3 m/s, all configurations begin generating more power. Although the curved flange setup continues to outperform the others, its percentage advantage begins to decrease. Nonetheless, it still offers clear benefits, confirming its effectiveness in moderate wind conditions. At 8.7 m/s, the differences in power output among the configurations become less pronounced. While the shroud with the curved flange still leads, the performance gap narrows. By 11.32 m/s, the power outputs of the shroud-plus-curved-flange and the

shroud-plus-vertical-flange configurations are nearly identical. This convergence suggests that at this wind speed, the aerodynamic benefits of the curved flange are diminished, possibly due to airflow dynamics that equalize performance between the two flange types. At 13.82 m/s, the performance curves of the curved and vertical flanges are virtually indistinguishable. This indicates that at higher wind speeds, the advantage of the curved flange diminishes further, making the choice of augmenter less critical. Finally, at the maximum tested wind speed of 16.35 m/s, the performance of both flange-equipped configurations becomes nearly identical, reinforcing the conclusion that the curved flange's primary advantage is at lower wind speeds. It is important to note that these results are specific to the turbine model used in this study. If a turbine optimized for higher wind speeds were employed, the curved flange might continue to offer a performance edge over a broader velocity range. Even at higher wind speeds—where the current turbine shows minimal differences between flange types—a high-speed-optimized turbine could better exploit the aerodynamic benefits of the curved flange. This suggests that the curved flange remains a valuable augmenter not only for low-wind urban applications but also for high-wind scenarios when paired with a turbine designed to match those conditions.

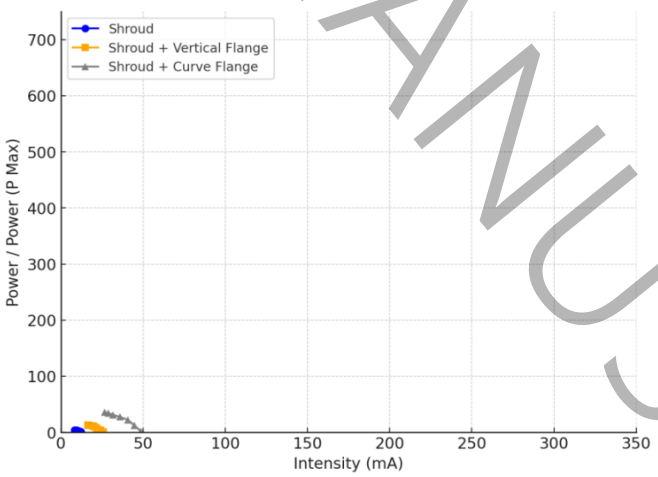

(a)

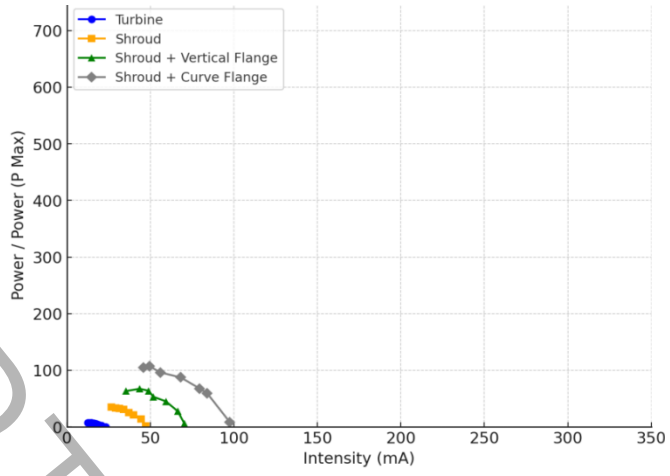

(b)

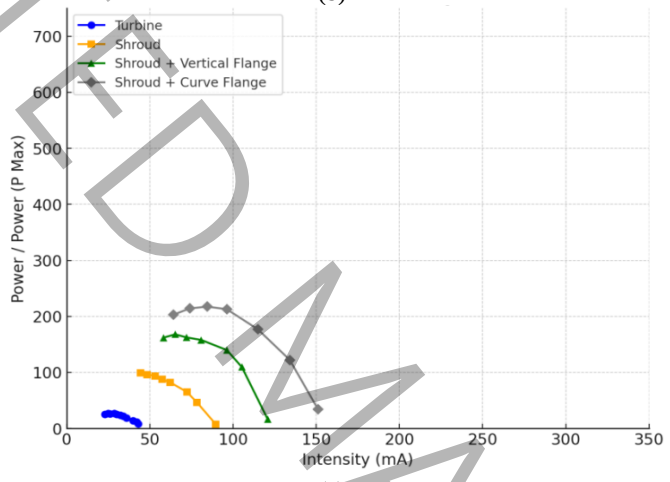

(c)

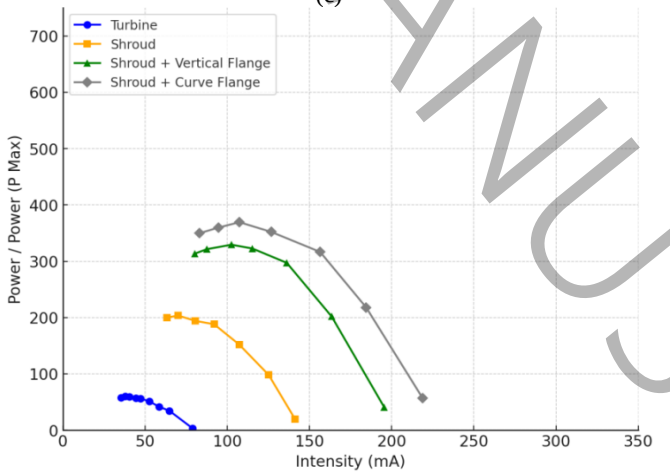

(d)

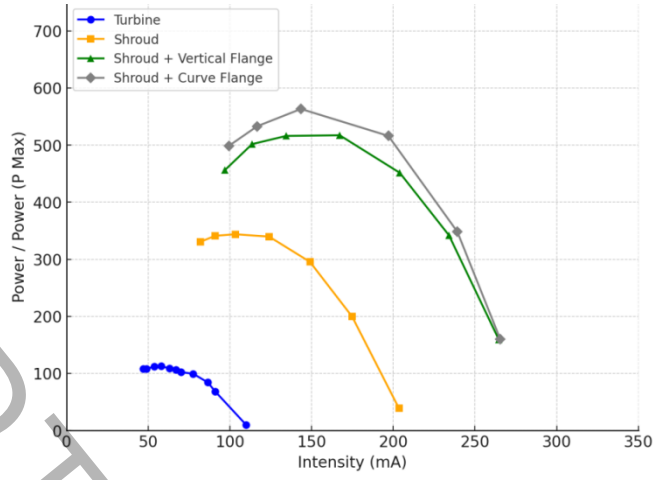

(e)

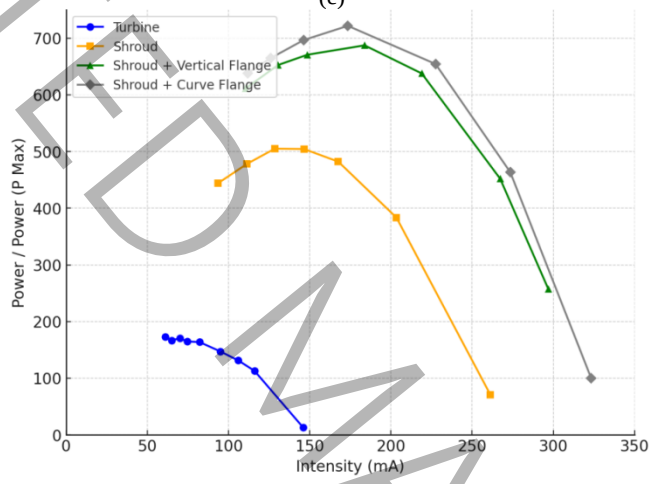

(d)

Fig. 9 Power changes with current intensity at free flow speeds (a) 3.8 m/s, (b) 6.3 m/s, (c) 8.7 m/s, (d) 11.32 m/s, (e) 13.82 m/s, (f) 16.35 m/s.

Table 3 compares the power output of a standalone turbine with that of the same turbine equipped with various augmenters—a shroud, a vertical flange, and a curved flange—across different wind speeds. The results highlight substantial gains in power, particularly at lower velocities, where augmentation is most impactful. At a low wind speed of 5 m/s, the bare turbine produces 1.416 units of power. Adding a shroud increases the output to 10.893 units, a 769.22% improvement. Incorporating a vertical flange boosts the power further to 23.560 units, representing a 1663.66% increase. The most significant enhancement occurs with the curved flange, elevating power output to 45.764 units, a 3231.56% increase over the standalone turbine. This dramatic gain emphasizes the critical role of aerodynamic augmentation—especially curved flanges—in low-Reynolds-number regimes, where bare turbines typically struggle to generate sufficient torque. At a medium wind speed of 7.5 m/s, the bare turbine delivers 10.134 units of

power. With a shroud, output rises to 45.060 units (444.62%), while the vertical flange increases it to 77.977 units (769.43%). The curved flange again proves most effective, raising power to 125.073 units, marking a 1234.13% improvement. Although still significant, the percentage gains are less dramatic than at lower speeds, indicating a tapering effect as natural aerodynamic efficiency improves. At a high wind speed of 16.35 m/s, the standalone turbine generates 138.077 units. The addition of a shroud increases this to 409.677 units (296.70%), while the vertical flange pushes output to 562.600 units (407.45%). The curved flange yields a comparable 567.221 units, reflecting a 410.80% gain. These results suggest that while augmenters remain effective at higher wind speeds, their relative impact diminishes as the turbine's inherent aerodynamic design becomes the dominant factor in power generation. Overall, the data demonstrate that augmenters, especially the curved flange, can lead to exponential improvements in power output at low wind speeds, making them essential in urban or low-wind regions where energy capture is challenging. As wind speeds rise, the relative advantage of augmenters decreases, and optimizing the turbine's aerodynamic profile becomes more important. Still, across all wind speeds tested, the curved flange consistently delivers the highest power output, followed by the vertical flange and then the shroud alone. This consistent performance makes the curved flange a highly effective design feature, both for enhancing airflow and reducing aerodynamic losses. Therefore, in regions with low to moderate wind speeds, integrating a curved flange into turbine design should be prioritized to maximize energy yield. In contrast, for high-wind environments, focusing on improving the turbine's blade and rotor design may yield greater efficiency, as the marginal benefits of augmentation taper off.

Table 3. Power comparison of alone turbine and with augmenters

Free stream velocity (m/s)	Alone turbine	Turbine + shroud	Turbine + shroud + vertical flange	Turbine + shroud + curved flange
3.8	-	2.61	8.53	23.64
5	1.41	10.89 (769.223%)	23.56 (1663.656%)	45.76 (3231.563%)
6.3	5.48	24.45 (445.666%)	46.65 (850.129%)	76.03 (1385.468%)
7.5	10.13	45.06 (444.641%)	77.97 (769.428%)	125.07 (1234.127%)
8.7	20.80	72.20 (347.150%)	130.88 (629.264%)	168.69 (811.049%)
9.9	30.22	110.51 (365.606%)	184.15 (609.239%)	225.96 (747.567%)
11.32	46.77	150.73 (322.235%)	260.94 (557.829%)	288.93 (617.675%)
12.55	63.46	207.63 (327.179%)	335.46 (528.596%)	373.15 (587.987%)
13.82	92.75	269.84 (290.906%)	420.55 (453.385%)	436.56 (470.643%)
15.08	121.03	339.09 (280.154%)	479.11 (395.837%)	515.23 (425.672%)
16.35	138.07	409.67 (296.701%)	562.60 (407.452%)	567.22 (410.799%)

4-13- Comparison of Average Turbine Power under Different Configurations and Wind Speeds

The average power output of the turbine was evaluated for four configurations. The bare turbine (without any flow enhancement) was considered the baseline. A simple shroud was tested in the second configuration, followed by a shroud with a vertical flange in the third configuration, and finally a shroud with an improved curved flange in the fourth configuration. Figs. 10(a–f) collectively demonstrate how the three shrouded configurations significantly enhance turbine performance relative to the bare turbine across all wind conditions. At a wind speed of 5.6 m/s (Fig. 10(a)), the bare turbine was unable to start and produced zero power. The simple shroud enabled an output of 5.9 mW, while adding a vertical flange increased the power to 19.3 mW (≈3.3× the simple shroud). The improved curved flange produced 53.4 mW, approximately 9× higher than the simple shroud. These results illustrate the crucial role of outlet geometry in reducing the startup threshold and enabling low-speed operation. At 6.3 m/s (Fig. 10(b)), all four configurations were operational. The bare turbine generated 3.26 mW, while the simple shroud

increased power to 24.6 mW. The vertical flange nearly doubled this value, reaching 53.2 mW. The improved curved flange achieved 103.4 mW, which is 31× the power of the bare turbine and nearly 2× the vertical flange. This reflects the strong Venturi effect and enhanced inflow acceleration from aerodynamic optimization. At 8.7 m/s (Fig. 10(c)), the performance trend continued. The bare turbine reached 12.4 mW, the simple shroud produced 55.3 mW (≈4.45×), and the vertical flange increased output to 105.4 mW. The improved curved flange delivered 171.8 mW, representing a 13.8-fold improvement over the bare turbine. Even at moderate wind speeds, the improved flange retains a substantial advantage. At 11.32 m/s (Fig. 10(d)), the bare turbine produced 68.4 mW, while the simple shroud reached 249.7 mW (≈3.65×). Adding the vertical flange boosted the power to 416.1 mW, and the improved curved flange further improved performance to 510.6 mW. The improved configuration provided 7.46× the power of the bare turbine and 1.23× that of the vertical flange, highlighting the continued benefit of flow-guiding structures at elevated wind speeds. At 13.82 m/s (Fig. 10(e)), the bare turbine generated 105.8 mW, while the simple shroud increased power to 340.6 mW. The vertical flange delivered 589.6 mW, and the improved curved flange achieved 652.9 mW, corresponding to more than 6× the bare turbine and 11% above the vertical-flange configuration. Even in high-speed regimes where power levels are generally high, the improved flange maintains a measurable performance advantage. At the highest examined wind speed of 16.35 m/s (Fig. 10(f)), the bare turbine produced 273 mW. The simple shroud increased output to 766.2 mW (≈2.8×), and the vertical flange further elevated it to 1082.6 mW. The improved curved flange yielded the highest performance with 1164.2 mW, corresponding to 4.26× the bare turbine and 1.08× the vertical flange. These results confirm that even at near-maximum operating efficiency, geometric optimization continues to deliver measurable gains.

Overall, the results across Figs. 10(a–f) show that shroud installation, particularly with an improved curved flange, not only lowers the startup threshold but also increases the extracted power at all wind speeds—ranging from several-fold improvements at low speeds to more than fourfold gains at high

speeds. This consistently demonstrates the strong influence of outlet geometry and aerodynamic optimization on wind-energy harvesting efficiency.

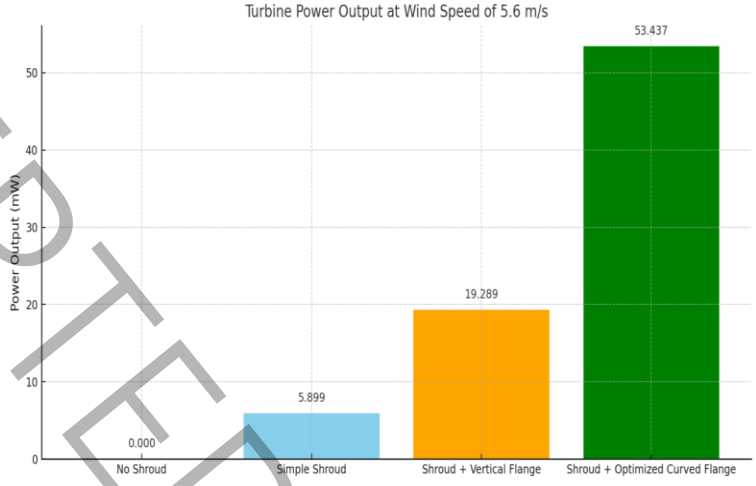

(a)

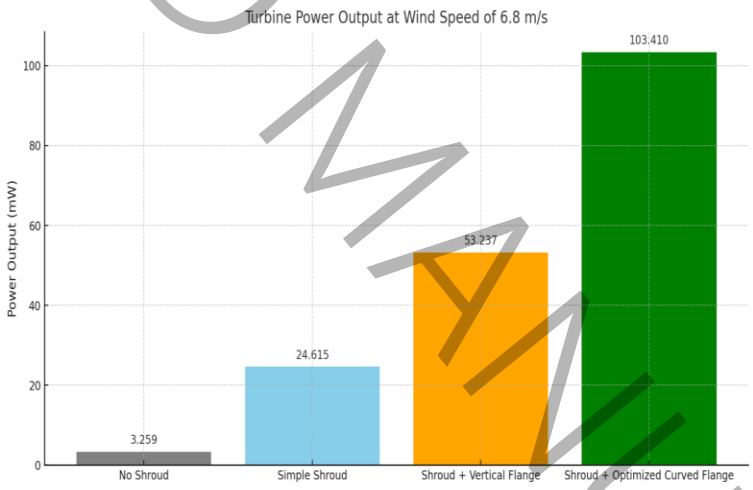

(b)

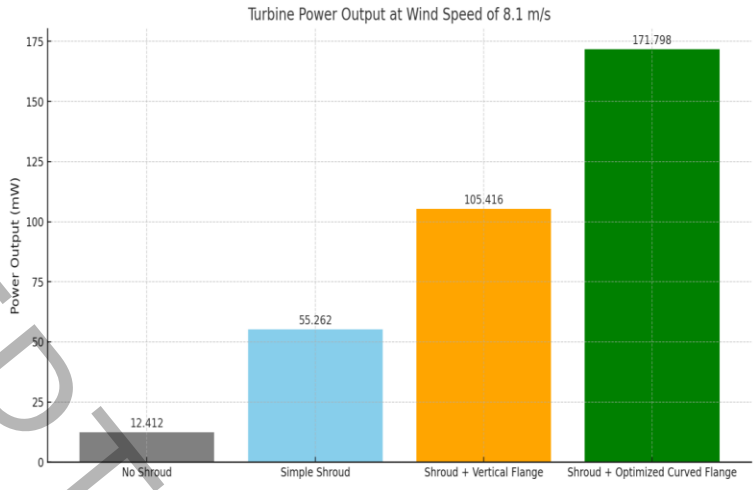

(c)

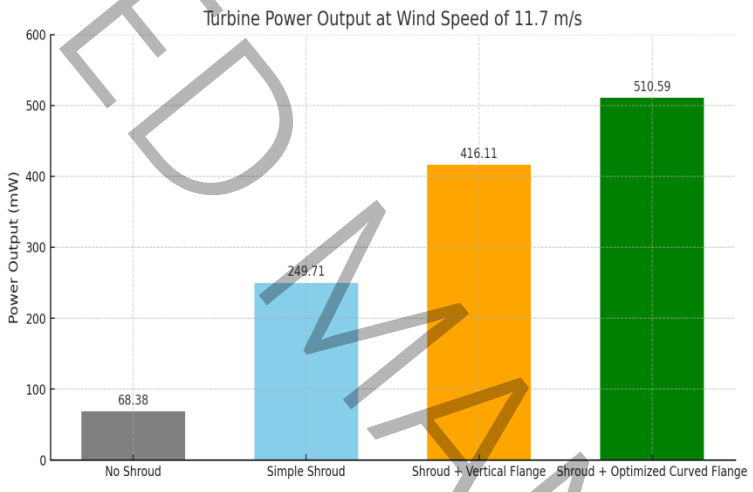

(d)

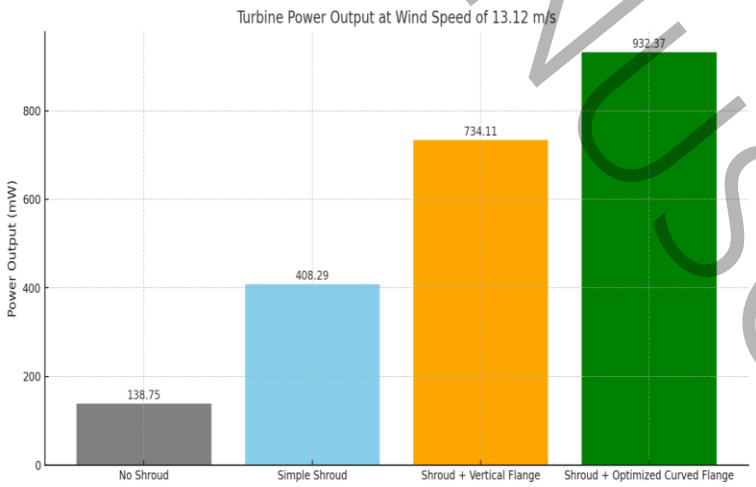

(e)

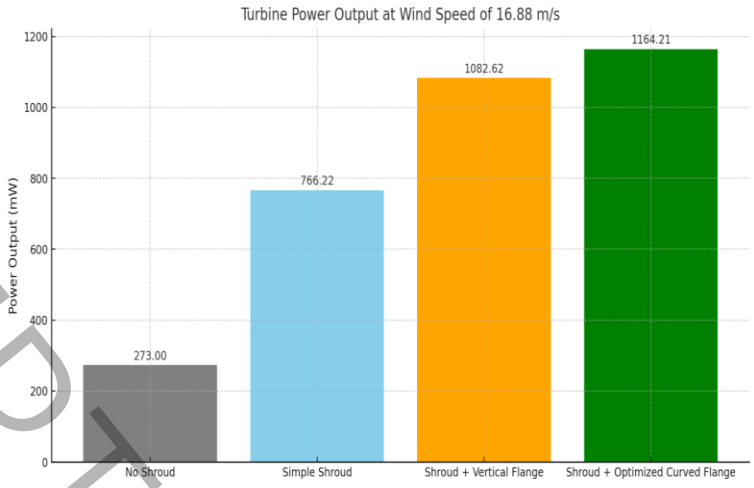

(f)

Fig 10. The average output power of the different turbine configurations, expressed in milliwatts, at the airspeeds of (a) 5.6, (b) 6.3, (c) 8.7, (d) 11.32, (e) 13.82 and (f) 16.37 m/s.

4-14- Evaluation of the Effect of the Shroud and Flange on the Average Power Output of the Wind Turbine

To investigate the influence of flow-enhancing components on the performance of the wind turbine under different electrical loads and wind speeds, Fig. 11 presents the average output power for the four turbine configurations. The results indicate that implementing a shroud alone leads to a significant increase in power output compared with the bare turbine. The average generated power of the bare turbine across all tested wind speeds was 222.91 mW, which increased to 325.96 mW when the simple shroud was added—an improvement of 46.2%. In the next stage, adding a vertical flange to the end of the shroud further increased the average power to 508.39 mW, corresponding to a 55.9% enhancement relative to the shroud without a flange and approximately 128.1% compared to the bare turbine. Finally, the curved-flange configuration, representing the improved aerodynamic design, achieved the highest average power of 578.19 mW. This value indicates an improvement of 13.7% over the vertical flange, 77.3% over the simple shroud, and 159.4% relative to the bare turbine.

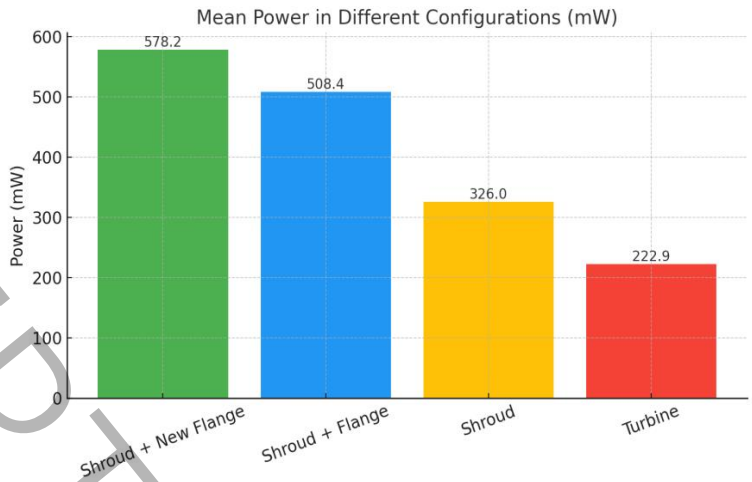

Fig 11. Average extracted power of the different configurations, expressed in milliwatts.

4-15- Limitations and Practical Considerations

While the proposed flange-enhanced shroud design demonstrates notable aerodynamic performance improvements in low-wind urban environments, several limitations should be acknowledged. Scaling the system for large-scale wind energy applications is constrained by both economic and structural considerations. The significant weight of a full-scale shroud, combined with the presence of naturally strong winds in typical wind farm locations, reduces the practicality of this approach for utility-scale deployment. Additionally, the increased aerodynamic drag caused by the flange requires more robust support structures, which can raise both construction and maintenance costs. In urban settings, further challenges may arise, such as spatial constraints, compliance with aesthetic and regulatory requirements, and the need for installation permits. These issues underscore the importance of context-specific evaluations when assessing the feasibility of implementing such designs in real-world scenarios.

5- Conclusion

This study comprehensively investigated the aerodynamic effects of enhanced curvature in wind turbine shroud flanges, focusing on their impact on airflow acceleration and turbine power output. All analyses demonstrated that the geometry of the flange, particularly its curvature and height, plays a critical role in optimizing airflow through the shroud throat. The improved curved-flange configuration consistently outperformed both the vertical-flange and shroud-only designs across a wide range of wind speeds, providing up to a 56.25% increase in throat velocity compared to the baseline vertical flange. These enhancements directly translated into substantial improvements in turbine performance, with power output gains exceeding 3,200% at low wind speeds and maintaining measurable advantages even at higher velocities. The results confirm that the curved flange effectively reduces startup thresholds, enhances inflow acceleration, and maximizes energy capture in low- to moderate-wind urban environments. Trend analyses further revealed that while vertical flanges offer limited benefits at low wind speeds, their effectiveness diminishes at higher velocities, whereas the curved flange maintains stable and consistent performance. Despite these promising findings, practical considerations—including structural weight, drag forces, and urban spatial constraints—must be addressed when implementing such designs. Overall, this research provides robust experimental evidence that integrating an improved curved flange into small-scale urban wind turbines substantially enhances aerodynamic efficiency and energy yield. The insights gained offer clear guidance for future turbine design and optimization, particularly for low-wind urban applications, while highlighting the potential limitations of scaling to utility-scale systems.

Conflict of Interest: The authors report no conflicts of interest.
Data Availability Statement: The data generated and analyzed in this study can be accessed upon reasonable request from the corresponding author.

Nomenclature

A	swept area of the turbine blades
C	Chord (mm)
Cp	pressure coefficient
Cpow	power coefficient

CFD	Computational Fluid Dynamics
DAWT	Diffuser Augmented Wind Turbine
DWT	Ducted Wind Turbine
MAE	Mean Absolute Error
NACA	National Advisory Committee for Aeronautics
NREL	National Renewable Energy Laboratory
P	Power (W)
Re	Reynolds number
Re_max	Maximum Reynolds number
RMS	Root Mean Square
RMSE	Root Mean Square Error
RSS	Root-Sum-Square
U	X-dir velocity component (ms^{-1})
u_i	velocity component in corresponding direction (ms^{-1})
V	Y-dir velocity component (ms^{-1})
$\vec{V}$	three-dimensional velocity vector
v	wind speed

References

[1] A.C. Aranake, V.K. Lakshminarayan, K. Duraisamy, Computational analysis of shrouded wind turbine configurations using a 3-dimensional RANS solver, Renewable Energy, 75 (2015) 818–832..

[2] A. Aranake, K. Duraisamy, Aerodynamic optimization of shrouded wind turbines, Wind Energy, 20(5) (2017) 877–889.

[3] A. Dilimulati, T. Stathopoulos, M. Paraschivoiu, Wind turbine designs for urban applications: A case study of shrouded diffuser casing for turbines, Journal of Wind Engineering and Industrial Aerodynamics, 175 (2018) 179–192.

[4] M. Shahsavarifard, E.L. Bibeau, Performance characteristics of shrouded horizontal axis hydrokinetic turbines in yawed conditions, Ocean Engineering, 197 (2020) 106916.

[5] N.K. Siavash, G. Najafi, T.T. Hashjin, B. Ghobadian, E. Mahmoodi, An innovative variable shroud for micro wind turbines, Renewable Energy, 145 (2020) 1061–1072.

[6]S.D. Karmakar, H. Chattopadhyay, A review of augmentation methods to enhance the performance of vertical axis wind turbine, Sustainable Energy Technologies and Assessments, 53 (2022) 102469.

[7]A. Ilhan, B. Sahin, M. Bilgili, A review: diffuser augmented wind turbine technologies, International Journal of Green Energy, 19(1) (2022) 1–27.

[8] R. Bontempo, E. Di Marzo, M. Manna, Diffuser augmented wind turbines: A critical analysis of the design practice based on the ducting of an existing open rotor, Journal of Wind Engineering and Industrial Aerodynamics, 238 (2023) 105428.

[9] W. Han, P. Yan, W. Han, Y. He, Design of wind turbines with shroud and lobed ejectors for efficient utilization of low-grade wind energy, Energy, 89 (2015) 687–701.

[10] B. Kosasih, A. Tondelli, Experimental study of shrouded micro-wind turbine, Procedia Engineering, 49 (2012) 92–98.
.

[11] N.A. Pambudi, R. Febriyanto, K.M. Wibowo, N.D. Setyawan, N.S. Wardani, L.H. Saw, B. Rudiyanto, The performance of shrouded wind turbine at low wind speed condition, Energy Procedia, 158 (2019) 260–265.

[12] B.A. Alquraishi, N.Z. Asmuin, S. Mohd, W.A. Abd Al-Wahid, A.N. Mohammed, Review on diffuser augmented wind turbine (dawt), International Journal of Integrated Engineering, 11(1) (2019).

[13] S.N. Akour, M.A.A. Mhaisen, Parametric design analysis of elliptical shroud profile, AIMS Energy, 9(6) (2021) 1147–1169.

[14] S.N. Leloudas, G.N. Lygidakis, A.I. Eskantar, I.K. Nikolos, A robust methodology for the design optimization of diffuser augmented wind turbine shrouds, Renewable Energy, 150 (2020) 722–742.

[15]Y. Ohya, T. Karasudani, A. Sakurai, K.-i. Abe, M. Inoue, Development of a shrouded wind turbine with a flanged diffuser, Journal of wind engineering and industrial aerodynamics, 96(5) (2008) 524–539.

[16] A. Niknahad, A. Khoshnevis, Numerical Investigation Of The Best Wind Turbine Shroud Flange Curvature For Maximum Wind Power Extraction, AUT Journal of Mechanical Engineering, 7(2) (2023) 185–198.

[17]M. Lipian, I. Dobrev, M. Karczewski, F. Massouh, K. Jozwik, Small wind turbine augmentation: Experimental investigations of shrouded-and twin-rotor wind turbine systems, Energy, 186 (2019) 115855.

[18]M. Lipian, I. Dobrev, F. Massouh, K. Jozwik, Small wind turbine augmentation: Numerical investigations of shrouded-and twin-rotor wind turbines, Energy, 201 (2020) 117588.

[19] M. Amin, H.H.M. ZoheirSaboohi, K.G. Osgouie, Investigation of the factors affecting the performance of Savonius wind turbine, Journal of Renewable Energy and New Energy, 10(2) (2023).

[20] S.E. Hosseini, Z. Saboohi, Ducted wind turbines: A review and assessment of different design models, Wind Engineering, (2024) 0309524X241282090.

[21] N. Maftouni, M. Taghaddosi, A CFD study of a flanged shrouded wind turbine: Effects of different flange surface types on output power, Scientia Iranica, 29 (1) (2022) 101–108.

[22] J.F. Hu, W.X. Wang, Upgrading a shrouded wind turbine with a self-adaptive flanged diffuser, Energies, 8 (6) (2015) 5319–5337.

[23] L. Gish, A. Carandang, G. Hawbaker, Experimental evaluation of a shrouded horizontal axis hydrokinetic turbine with pre-swirl stators, Ocean Engineering, 204 (2020) 107252.

[24] M.L. Hossain, S.N. Shams, S.M. Ullah, Comparative study of machine learning algorithms for wind speed prediction in Dhaka, Bangladesh, Sustainable Energy Research, 11(1) (2024) 23.

[25]Q. Zhang, D. Zhou, D. Xu, A. Rogora, Association between wind environment and spatial characteristics of high-rise residential buildings in cold regions through Field Measurements in Xi'an, Buildings, 13(8) (2023) 2007.

[26] K. Piasecki, E. Żmudzka, Severe storms as an example of a natural hazard in the urban area-case studies of the area of Warsaw, Poland, Miscellanea Geographica. Regional Studies on Development, 26(1) (2022) 63–74.

[27] V. Ok, M. Aygün, The variations of wind speeds with building density in urban areas, Architectural Science Review, 38(2) (1995) 87–95.